Spectrochimica Acta Part A: Molecular and Biomolecular Spectroscopy 257 (2021) 119789

Contents lists available at ScienceDirect

Spectrochimica Acta Part A: Molecular and Biomolecular Spectroscopy

journal homepage: www.elsevier.com/locate/saa

A bifunctional fluorescent probe for simultaneous detection of GSH and H_2S_n (n > 1) from different channels with long-wavelength emission

Peixin Niu [a], Yifan Rong [a], Yuyue Wang [a], Huijie Ni [a], Minghui Zhu [a], Wenqiang Chen [c], Xingjiang Liu [a,*], Liuhe Wei [a], Xiangzhi Song [b]

[a] Green Catalysis Center, College of Chemistry, Zhengzhou University, Zhengzhou 450001, Henan Province, China
[b] College of Chemistry & Chemical Engineering, Central South University, Changsha 410083, Hunan Province, China
[c] Guangxi Key Laboratory of Natural Polymer Chemistry and Physics, Nanning Normal University, Nanning 530001, Guangxi Province, China

HIGHLIGHTS

- A bifunctional fluorescent probe, DCM-Cou-SePh, for simultaneous detection of GSH and H_2S_n (n > 1) from different channels were developed.
- This probe displayed long-wavelength emissions in detection of GSH and H_2S_n (GSH: $\lambda_{ex/em}$ = 430/530 nm, H_2S_n: $\lambda_{ex/em}$ = 560/680 nm).
- This probe exhibited low detection limits for the detection of GSH and H_2S_n (0.12 μM for GSH, 0.19 μM for H_2S_n).
- This probe was capable of distinguishing endogenous GSH and H_2S_n (n > 1) in living cells.

GRAPHICAL ABSTRACT

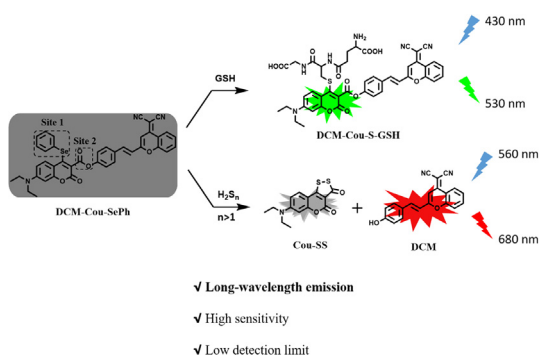

ARTICLE INFO

Article history:
Received 25 January 2021
Received in revised form 2 April 2021
Accepted 2 April 2021
Available online 08 April 2021

Keywords:
Glutathione
Polysulfide
Long-wavelength emission
Cell imaging
Fluorescent probe

ABSTRACT

In this work, we presented a long-wavelength emission fluorescent probe **DCM-Cou-SePh** that can discriminatively detect glutathione (GSH) and hydrogen polysulfides (H_2S_n, n > 1) from green and red emission channels, respectively. With the addition of GSH, probe **DCM-Cou-SePh** displayed green fluorescence emission ($\lambda_{ex/em}$ = 430/530 nm). In the presence of H_2S_n, the probe exhibited a significant fluorescence enhancement in red channel ($\lambda_{ex/em}$ = 560/680 nm). We also demonstrated that this probe was suitable to quantitatively detect GSH and H_2S_n with low detection limits (0.12 μM for GSH, 0.19 μM for H_2S_n). Furthermore, **DCM-Cou-SePh** can be used for sensing endogenous GSH and H_2S_n in living cells by dual-color fluorescence imaging.

1. Introduction

Reactive sulfur species (RSS), a group of sulfhydryl-containing compounds, generally exist in biological systems [1–3]. These thiol-containing molecules coordinately adjust various physiological and pathological processes to maintain the normal function of

* Corresponding author.
E-mail address: xingjiangliu@zzu.edu.cn (X. Liu).

https://doi.org/10.1016/j.saa.2021.119789
1386-1425/

body [4–6]. The abnormal change of RSS may be a signal of certain diseases [1,5,7–13], such as Alzheimer's disease, hypertension, cardiovascular disease and liver cirrhosis. The typical RSS, GSH and H_2S_n, play essential roles in redox biology [14–17] and pathological processes [5,18–30]. In recent years, increasing numbers of studies have reported that these two species are deeply related in lots of physiological processes [31–34] and endogenous H_2S_n can be biosynthesized from GSH (sulfur source) through cystarhionine-γ-lyase (CSE) [9,35]. In order to reveal the interaction between GSH and H_2S_n in cellular activity, it is highly valuable to develop methods that can simultaneously differentiate GSH and H_2S_n in the same situation. However, it is challenging to simultaneously sense GSH and H_2S_n because of their similar structure and reaction reactivity.

Fluorescent probe, for its unique functions and features such as noninvasive, high-resolution, highly sensitive and real-time detection, has been widely developed and employed in monitoring and imaging all kinds of analytes [36–43]. In recent years, a lot of fluorescent sensors or probes for sensing of GSH or H_2S_n have been prepared and reported [44–56]. But most of them only can response to one analyte at a time from single-channel. Such probes fail to simultaneously detect and image GSH and H_2S_n under the same condition. One simple way gets around this problem is to use two specific probes at the same time [57,58]. However, such method not only has the flaw of larger invasive effects, but also brings potential interference between the two selected probes [59–62]. Thus, it is desired to develop a single-molecule fluorescent probe for simultaneously detecting GSH and H_2S_n from different channels. Especially, the bifunctional fluorescent probes with long-wavelength emission are more expect, because the long-wavelength emission has strong tissues penetration force and can also reduce the interference of auto-fluorescence aroused by cell components.

In this work, we designed and synthesized a dual-detection probe **DCM-Cou-SePh** with long-wavelength emission. This probe was constructed by connecting coumarin derivative (**Cou**) with phenylselenide moiety (**-SePh**), recognition site 1 and dye **DCM** through ester bond serves as site 2 (synthetic route shown in Scheme 1). We expected this probe exhibited green fluorescence in the presence of GSH and red fluorescence when treated with H_2S_n. We also demonstrated that probe **DCM-Cou-SePh** can be used as a detector to simultaneously image intracellular GSH and H_2S_n, and this probe was also capable of detecting endogenously produced H_2S_n.

2. Experimental

2.1. Instruments and materials

The reagents used in the experiment were purchased from commercial suppliers. Unless otherwise specified, all reagents were used without further purification. The distilled water was used in synthesis and fluorescent measurements. Use Bruker 400 NMR to record ^{1}H NMR and ^{13}C NMR spectra by TMS as an internal standard. The solution with different pH values were prepared by a Leici PHS-3C meter. HRMS spectra were obtained by Aglient 7250 and Waters UPLC G2-XS. The emission spectra were recorded on a Hitachi F-4600 fluorescence spectrometer. Uv–vis spectrometer (Puxi TU-1901, Beijing) was used to record absorption spectra. Cell imaging experiments were carried out on Olympus FV1000 confocal microscope.

2.2. Synthesis of 2, 4, DCM and Cou-SePh

Based on the reported literature procedures [63,64], compound **2** and **DCM** were prepared. According to the literature methods [65], we synthesized compound **4** and **Cou-SePh**.

2.3. Synthesis of DCM-Cou-SePh

Dye **DCM** (0.687 g, 2.2 mmol), coumpound **Cou-SePh** (0.835 g, 2.0 mmol), EDC (0.421 g, 2.2 mmol) and DMAP (0.269 g, 2.2 mmol) were dissolved in 5.0 mL anhydrous dichloromethane. The resulting reaction mixture was stirred for 5 h at room temperature under nitrogen atmosphere. After removal of organic solvent, using silica gel chromatography to purify the aimed product from the crude product using dichloromethane (DCM) / ethyl acetate (EA) as eluent (v/v, 10:1). Finally we obtained probe **DCM-Cou-SePh**, as an orange solid (0.745 g, yield 52.4%). ^{1}H NMR (400 MHz, $CDCl_3$) δ_H 8.95 (d, J = 8.4 Hz, 1H), 7.78 (t, J = 7.2 Hz, 1H), 7.71 (d, J = 9.1 Hz, 1H), 7.68–7.61 (m, 4H), 7.60–7.55 (m, 2H), 7.49 (t, J = 7.8 Hz, 1H), 7.32 (s, 1H), 7.30 (t, J = 3.1 Hz, 3H), 7.29 (s, 1H), 6.91 (s, 1H), 6.82 (d, J = 16.0 Hz, 1H), 6.51 (d, J = 9.1 Hz, 1H), 6.49 (d, J = 2.4 Hz, 1H), 3.43 (q, J = 7.1 Hz, 4H), 1.23 (t, J = 7.1 Hz, 6H).^{13}C NMR (100 MHz, $CDCl_3$) δ_C 163.4, 157.6, 157.3, 155.5, 152.9, 152.3, 151.9, 137.9, 134.7, 132.6, 131.3, 129.8, 129.6, 128.1, 126.0, 125.8, 122.6, 119.8, 119.0, 118.9, 118.7, 117.8, 116.8, 115.7, 109.5, 108.5, 107.1, 97.1, 63.0, 45.0, 12.5. HRMS (ESI) m/z: calcd. for $C_{40}H_{30}N_3O_5$-Se $[M + H]^+$ 712.1351, found 712.1350.

2.4. Cell culture and imaging

MGC-803 cells and RAW264.7 cells were cultured in CMEM medium containing 1% penicillin and 10% fetal bovine serum (FBS). The cultivation conditions of cells were as follows: culture temperature 37 °C, atmosphere containing 5% CO_2 and culture time 24 h. Before imaging experiments, the cells were washed by PBS buffer for three times. For the purpose of investigating the capability of the probe to image intracellular GSH and Na_2S_2, three group experiments were carried out using MGC-803 cells: A) For imaging GSH, the cells were incubated with probe **DCM-Cou-SePh** (10.0 μM) for 30 min. B) For imaging Na_2S_2, the cells were pre-cultured

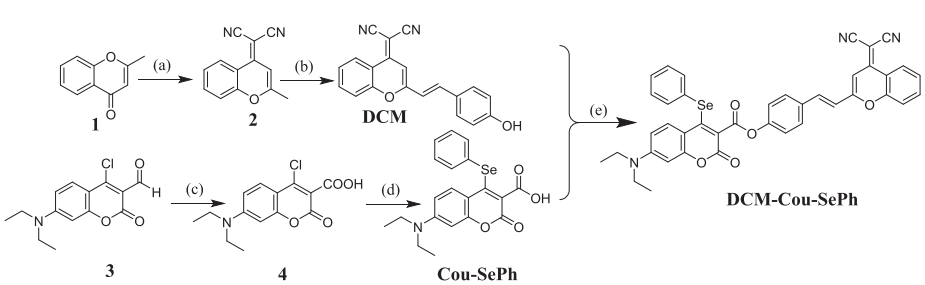

Scheme 1. The synthetic route of probe **DCM-Cou-SePh.** (a) malononitrile, acetic anhydride, reflux 10 h, yield 39.3%; (b) 4-hydroxybenzaldehyde, piperazine, acetic acid, methylbenzene, reflux 6 h, yield 42.7%; (c) resorcinol, $NaClO_2$, NaH_2PO_4, H_2O, 0 °C, 30 min, yield 76.2%; (d) phenylselenol, DMF, Et_3N, 25 °C, 20 min, yield 98.0%; (e) EDC, DMAP, DCM, rt, 5 h, yield 52.4%.

with Na_2S_2 (220.0 μM) for 15 min and then incubated with the probe (10.0 μM) for 30 min. C) As a control experiment, the cells were pretreated by *N*-ethylmaleimide (NEM, 1.0 mM) for 15 min and then treated with the probe (10.0 μM) for 30 min. In the imaging experiments of endogenous Na_2S_2, we conducted two group of experiments: A) After pretreated with 1.0 g/mL lipopolysaccharide (LPS), the RAW264.7 cells were treated with NEM (1.0 mM) for 15 min. Next, the cells were incubated with cystine (200.0 μM) for 30 min and finally treated with this probe (10.0 μM) for another 30 min. B) As a control experiment, the RAW264.7 cells were pretreated with NEM (1.0 mM) for 15 min and then incubated with cystine (200.0 μM) for another 30 min. Finally, the cells were treated with probe **DCM-Cou-SePh** (10.0 μM) for 30 min.

2.5. Detection limit

The detection limit was calculated according to the following equation:

$$\text{Detection limit} = 3\sigma/k$$

where σ is the standard deviation of blank measurement, k is the slope between fluorescence intensity versus GHS/Na_2S_2 concentration.

3. Results and discussion

3.1. Molecular design of DCM-Cou-SePh

For the above-mentioned considerations, we developed a fluorescent probe, **DCM-Cou-SePh**, for simultaneous detection of GSH and H_2S_n. The sensing mechanism of probe **DCM-Cou-SePh** for distinguishing RSS was shown in Scheme 2. This probe contains two dyes connected with an ester bond: dye 7-diethylaminocoumarin (**Cou**) and (2-(4-hydroxystyryl)-4H-chromen-4-ylidene) malononitrile (**DCM**). Both of them displayed excellent optical properties [63,65]. Particularlu, dye **DCM** emitted deep red fluorescence with emission band centered at 680 nm. The emission spectra of them were well-separated (**Cou**: λ_{em} = 515 nm, **DCM**: λ_{em} = 680 nm) (Fig. S1), which can enable to provide different fluorescence signal patterns to sense GSH and H_2S_n from different emission channels. There are two recognition sites in **DCM-Cou-SePh**. For site 1, the benzeneselenol moiety not only acts as an effective group to quench fluorescence of this probe *via* photo-induced electron transfer (PET) process [66,67], but also plays the action of leaving group through S_NAr reaction. Moreover, the ester bond (site 2) between **DCM** and **Cou** functions as another recognition factor to realize the distinguishing of H_2S_n over other RSS. When **DCM-Cou-SePh** was treated with GSH, thiol group of GSH as a nucleophile agent, would directly attack benzeneselenol moiety to generate the green-emitting sulfur-substitued **DCM-Cou-S-GSH** *via* S_NAr substitution reaction. Similarly, when this probe was incubated with Cys/Hcy, site 1 can be cut off to give **DCM-Cou-S-Cys/Hcy** by S_NAr substitution reaction. However, the intermediate **DCM-Cou-S-Cys/Hcy** can be converted to corresponding nonfluorescent amino-substituted derivatives **DCM-Cou-N-Cys/Hcy** through intermolecular rearrangement. Treatment of **DCM-Cou-SePh** with H_2S_n was expected to rapidly replace the phenylselenide moiety *via* a S_NAr displacement to obtain **DCM-Cou-SSH**. Subsequently, the initially formed **DCM-Cou-SSH** can undergo a further intramolecular cyclization between the the ester group (site 2) and thiol group to release the red-emitting dye **DCM** and the nonfluorescent coumarindithiolone (**Cou-SS**). H_2S may react with this probe to generate a nonfluorescent compound, **DCM-Cou-SH** by S_NAr mechanism. Therefore, this probe could selectively detect GSH and H_2S_n over other RSS from different channels.

3.2. Sensitivity study

To investigate the sensitivity of **DCM-Cou-SePh** toward GSH and Na_2S_2, the fluorescence titration spectra of this probe were studied in PBS buffer (10.0 mM, pH = 7.4, containing 1.0 mM CTAB)

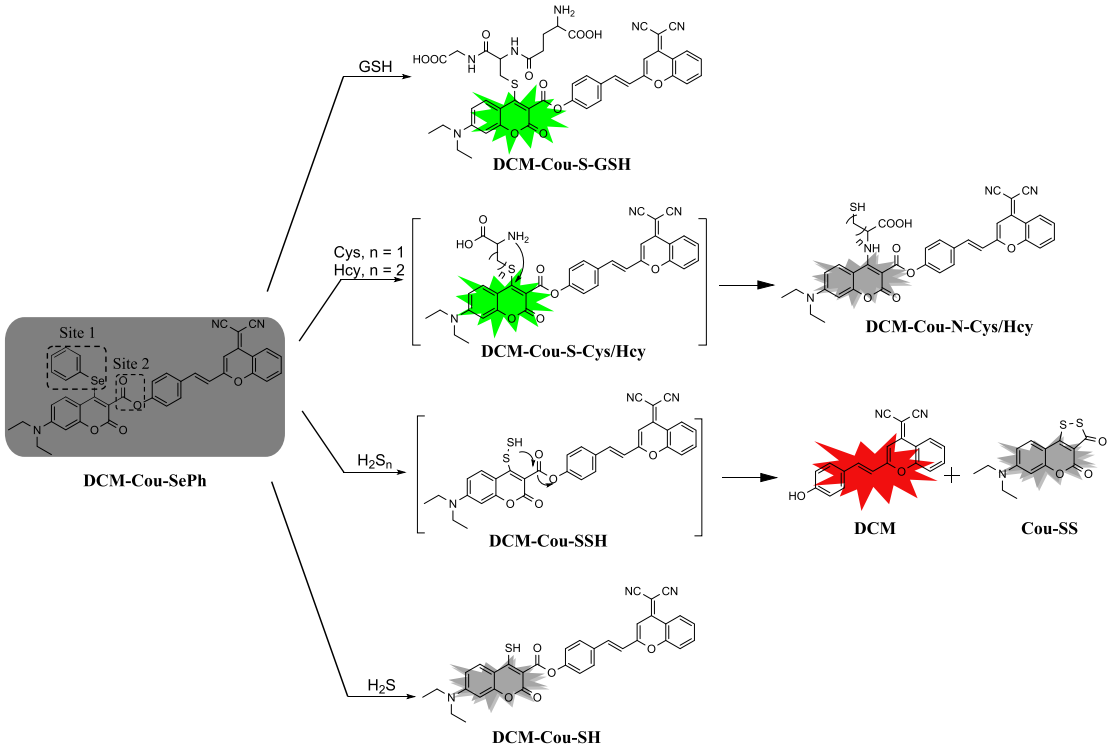

Scheme 2. The sensing mechanism of probe DCM-Cou-SePh for distinguishing RSS.

at 25 °C. Firstly, the fluorescence quantum yield of this probe was determined in the test system, and as expected the solution of this probe exhibited a low quantum yield (0.17%). The solution of this probe (10.0 μM) subjected to an obvious emission enhancement with λ_{em} = 530 nm upon gradual addition of GSH (Fig. 1A1), and fluorescence intensity at 530 nm ($I_{530\ nm}$) enhanced with the increasing amount of GSH and reached the maximum when 1.4 equiv. of GSH was added. $I_{530\ nm}$ was linear with the concentration of GSH in the range of 0.0–4.0 μM with good linear correlation coefficient (R = 0.9994). To our delight, this probe displayed low detection limit for GSH (0.12 μM) when the ratio of signal to noise is 3 (Fig. 1A2). In the case of Na_2S_2, an obvious emission band centered at 680 nm can be observed and the emission intensity enhanced with the rising of concentration of Na_2S_2 (Fig. 1B1). The intensity can reach equilibrium when 22.0 equiv. of Na_2S_2 was added. Furthermore, a good linear relationship (R = 0.9945) between $I_{680\ nm}$ and the concentrations of Na_2S_2 was found in the range of 0.0–220.0 μM with a 0.19 μM detection limit based on S/N = 3 (Fig. 1B2). As consequence, probe **DCM-Cou-SePh** was able to distinguish GSH and Na_2S_2 from green and red emission channels with good sensitivity.

3.3. Kinetic study

Time-dependent fluorescence experiments of probe **DCM-Cou-SePh** toward GSH/Na_2S_2 were performed in PBS buffer (10.0 mM, pH = 7.4, containing 1.0 mM CTAB) at 25 °C. When the probe (10.0 μM) was treated with 1.4 equiv. of GSH, the fluorescence emission at 530 nm increased immediately and achieved the balance within 9 min (Fig. 2a). After addition of 22.0 equiv. of Na_2S_2 to the solution of the probe (10.0 μM), the fluorescence intensity at 680 nm increased with time and reached the peak value at 30 min (Fig. 2b). The intensity at 530 nm and 680 nm of the free probe had no significant changes under the same experiment condition. These experiment results clearly stated that probe **DCM-Cou-SePh** possessed a good stability and could rapidly response to GSH and H_2S_n.

3.4. Selectivity study

To investigate the selectivity of probe **DCM-Cou-SePh**, the fluorescence behaviors of the probe (10.0 μM) responding to various potential analytes (NaCl, KCl, $CaCl_2$, $ZnCl_2$, $MgCl_2$, NaClO, $Na_2S_2O_3$, $NaSO_3$, $NaHSO_3$, Na_2SO_4, Na_2S, H_2O_2, L-Pro, L-Ser, L-Glu, DL-Tyr, Cys, Hcy, GSH and Na_2S_2) were examined in PBS buffer (10.0 mM, pH = 7.4, 1.0 mM CTAB). As shown in Fig. 3, comparison of fluorescence emission spectra before and after treatment with analytes showed that only GSH and Na_2S_2 can generate significant fluorescence enhancement. Overall, the results confirmed that probe **DCM-Cou-SePh** exhibited high selectivity to GSH and H_2S_n over other potential interfering species.

3.5. Effect of pH

In order to evaluate whether probe **DCM-Cou-SePh** can work under physiological environment, the fluorescence patterns of the probe (10.0 μM) with GSH/Na_2S_2 were studied in different pH buffer solutions. The measurements were depicted in Fig. S2. According to the study, we found that the fluorescence change at 530 nm and 680 nm of this probe can be neglected in pH range from 2.0 to 10.0, suggesting that this probe can keep stable in a wide pH range. Upon treatment with GSH, the fluorescence signal at 530 nm displayed remarkable enhancement in the pH range from 7.0 to 12.0. In the case of Na_2S_2, we observed the fluorescence value at 680 nm enhanced significantly in the pH range of 7.0–10.0. These experiment results proved that this probe had the potential to be used for simultaneously sensing GSH and H_2S_n under physiological environment.

3.6. Responding mechanism study

In order to verify the response mechanism of the probe, HRMS analysis was carried out on the reaction mixtures of **DCM-Cou-SePh** with GSH and Na_2S_2. As shown in Fig. S6, the mixture of **DCM-Cou-SePh** with GSH displayed an obvious peak at

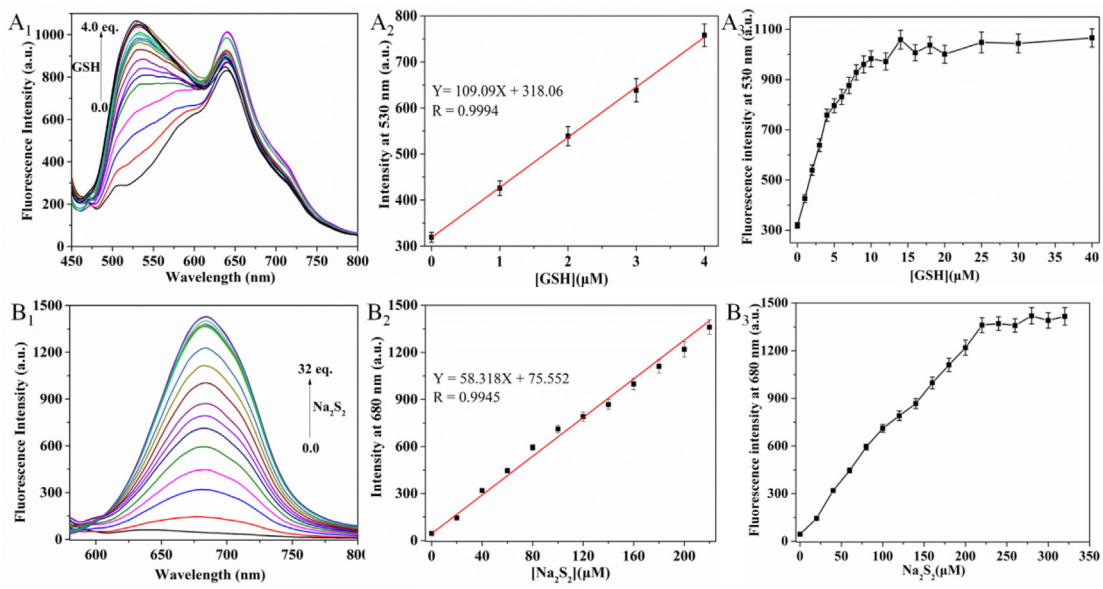

Fig. 1. (A_1-B_1) Fluorescence spectra of DCM-Cou-SePh (10.0 μM) was treated with different concentrations of GSH (0.0–4.0 equiv.) and Na_2S_2 (0.0–32.0 equiv.). (A_2-B_2) Linear correlation between concentrations of GSH/Na_2S_2 and fluorescence intensity (530 nm and 680 nm). (B_3-B_3) Fluorescence spectra changes of DCM-Cou-SePh (10.0 μM) upon addition GSH (0.0–4.0 equiv.) and Na_2S_2 (0.0–32.0 equiv.). Data were recorded in PBS buffer (10.0 mM, pH = 7.4, 1.0 mM CTAB) at 25 °C. (A_1-A_2) Excited at 430 nm, (B_1-B_2) Excited at 560 nm.

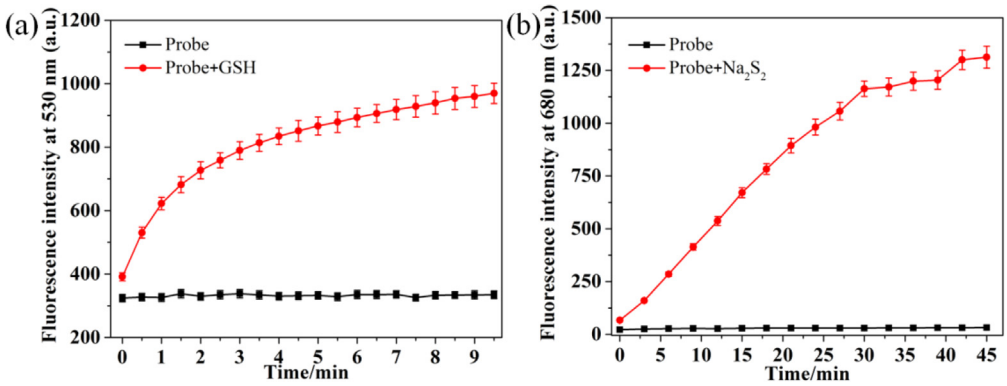

Fig. 2. Time-dependent fluorescence intensitiy at 530 nm and 680 nm for probe **DCM-Cou-SePh** (10.0 μM) with (a) GSH (1.4 equiv.) and (b) Na_2S_2 (22.0 equiv.) respectively. Data were recorded in PBS buffer (10.0 mM, pH = 7.4, 1.0 mM CTAB) at 25 °C. (a) Excited at 430 nm, (b) Excited at 560 nm.

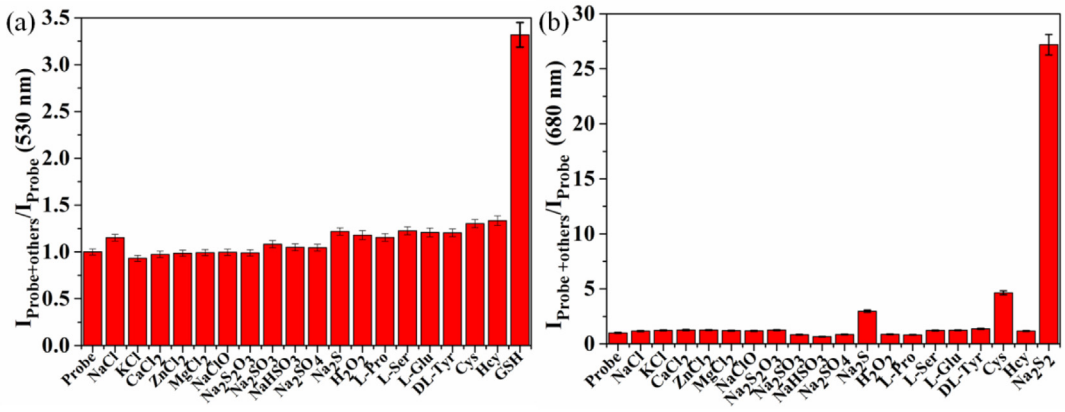

Fig. 3. The ratio of fluorescence intensity of probe **DCM-Cou-SePh** (10.0 μM) at 530 nm for GSH and 680 nm for Na_2S_2 upon treatment with various analytes respectively. Data were recorded in PBS buffer (10.0 mM, pH = 7.4, 1.0 mM CTAB) at 25 °C. (a) Excited at 430 nm, (b) Excited at 560 nm. The concentration of each analyte: 14.0 μM in the experiment for GSH, 220.0 μM in the experiment for Na_2S_2.

861.2547, which was practically identical to the mass weight of **DCM-Cou-S-GSH** (calcd. for $C_{44}H_{41}N_6O_{11}S$ $[M+H]^+$, m/z = 861.2554). As shown in Fig. S7, for Na_2S_2, two peaks at 308.0423 and 313.0968 were found, corresponding to **Cou-SS** (calcd. for $C_{14}H_{14}NO_3S_2$ $[M+H]^+$, m/z = 308.0415) and **DCM** (calcd. for $C_{20}H_{13}N_2O_2$ $[M+H]^+$, m/z = 313.0977). The experimental results clearly and convincingly supported the proposed sensing mchanism.

3.7. Cell imaging

Firstly, we performed MTT assays on probe **DCM-Cou-SePh** to evaluate its cytotoxicity to HeLa cells. As shown in Fig. S10, the survival rate for this probe at the concentration below 20.0 μM is up to 93% after incubation for 24 h, indicating that this probe had a low cytotoxicity to living cells. It was proved that the applied potential of this probe in biological system.

To verify the capability of probe **DCM-Cou-SePh** to image intracellular GSH and Na_2S_2, cell imaging experiments were conducted. As shown in Fig. 4A1-A4, when MGC-803 cells were only treated with the probe (10.0 μM) for 30 min, we observed strong green fluorescence and very weak red fluorescence from different channels, which showed that this probe was responsive to intracellular GSH. For the imaging of H_2S_2, red channel displayed strong fluorescence and green channel emitted faint fluorescence when the cells were pretreated with Na_2S_2 (220.0 μM) for 15 min and futher treated with the probe (10.0 μM) for 30 min (Fig. 4B1-B4). For the control experiment, very weak fluorescence was observed in two emission channels when this probe (10.0 μM) was treated with the NEM-pretreated cells for 30 min (Fig. 4C1-C4). These cell experiments studies showed that this probe could be applied in the discrimination of intracellular GSH and H_2S_n in living cells.

Then, we set out to perform the experiments of the imaging endogenous H_2S_n in living RAW264.7 cells. According to the reported methods, cystathionine-γ-lyase (CSE) can induce cells to produce endogenous H_2S_n using cystine as sulfur source [17,65,68]. In the experimental group, cells were pretreated for 8 h with 1.0 μg/mL lipopolysaccharide (LPS, stimulate the overexpression of the CSE mRNA in cells), further treated with *N*-ethylmaleimide (NEM, 1.0 mM) for 15 min, then incubated with cystine (200.0 μM) for 30 min, and finally incubated with this probe (10.0 μM) for another 30 min. The imaging results were shown in Fig. 5A1-A4, an obvious red fluorescent signal and a faint green fluorescent signal can be observed. As for the control group, RAW264.7 cells were cultured with NEM (1.0 mM) at first, and then incubated with cystine (200.0 μM) and the probe (10.0 μM), successively. Both the green and red channels emitted very weak fluorescence. These imaging experiments confirmed that this probe could image endogenous H_2S_n in living cells.

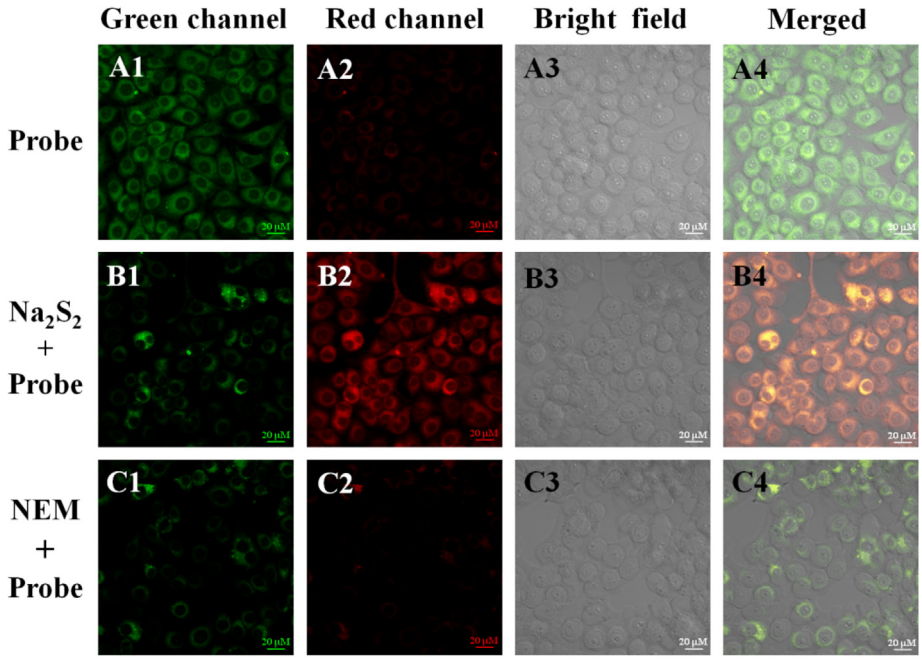

Fig. 4. Fluorescence images of GSH and H_2S_n in living MGC-803 cells. (A1-A4) Cells only incubated with **DCM-Cou-SePh** (10.0 μM) for 30 min; (B1-B4) Cells treated with Na_2S_2 (220.0 μM) for 15 min and then incubated with **DCM-Cou-SePh** (10.0 μM) for 30 min; (C1-C4) NEM-pretreated cells incubated with **DCM-Cou-SePh** (10.0 μM) for 30 min. Green channel: λ_{ex} = 405 nm, emissions were collected at 500–550 nm. Red channel: λ_{ex} = 543 nm, emissions were collected at 650–700 nm.

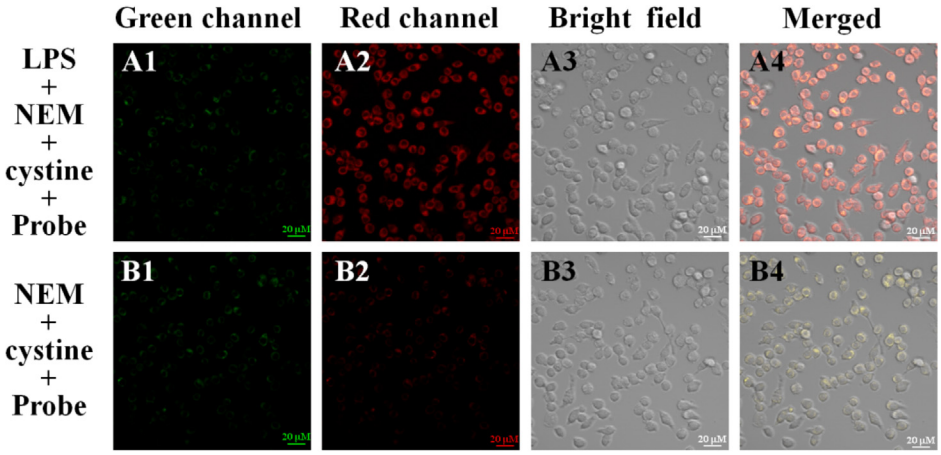

Fig. 5. Fluorescence images of endogenous H_2S_n in RAW264.7 cells. (A1-A4) Cells were pretreated with 1 μg/mL LPS for 8 h, NEM (1.0 mM) for 15 min, cystine (200.0 μM) for 30 min and then incubated with DCM-Cou-SePh (10.0 μM) for 30 min, (B1-B4) Cells were pretreated with NEM (1.0 mM) for 15 min, cystine (200.0 μM) for 30 min and fianlly treated with probe (10.0 μM) for 30 min. Green channel: λ_{ex} = 405 nm, emissions were collected at 500–550 nm. Red channel: λ_{ex} = 543 nm, emissions were collected at 650–700 nm.

4. Conclusions

In summary, a long-wavelength emission fluorescent probe, **DCM-Cou-SePh** was developed for distinguish GSH and H_2S_n (n > 1) from different fluorescence emission channels (GSH: $\lambda_{ex/em}$ = 430/530 nm, H_2S_n: $\lambda_{ex/em}$ = 560/680 nm). This probe displayed good stability, good selectivity and high sensitivity during the simultaneous detection of GSH and H_2S_n. This probe also can quantitatively detect GSH and H_2S_n with low detection limits, 0.12 μM for GSH and 0.19 μM for H_2S_n respectively. The capability of probe **DCM-Cou-SePh** for simultaneously sensing intracellular GSH and H_2S_n in living cells was successfully demonstrated by cell imaging experiments. Moreover, this probe was capable of imaging endogenously produced H_2S_n.

CRediT authorship contribution statement

Peixin Niu: Writing - original draft, Investigation. **Yifan Rong:** Writing - original draft, Investigation, Data curation. **Yuyue Wang:** Investigation. **Huijie Ni:** Investigation. **Minghui Zhu:** Investigation. **Wenqiang Chen:** Writing - review & editing, Formal analysis. **Xingjiang Liu:** Conceptualization, Supervision, Funding acquisition. **Liuhe Wei:** Project administration, Resources. **Xiangzhi Song:** Writing - review & editing.

Declaration of Competing Interest

The authors declare that they have no known competing financial interests or personal relationships that could have appeared to influence the work reported in this paper.

Acknowledgements

This research was supported by the National Natural Science Foundation of China (No.22008222).

Appendix A. Supplementary material

Supplementary data to this article can be found online at https://doi.org/10.1016/j.saa.2021.119789.

References

[1] C.E. Paulsen, K.S. Carroll, Cysteine-mediated redox signaling: chemistry, biology, and tools for discovery, Chem. Rev. 113 (2013) 4633–4679.
[2] X. Yang, L. He, K. Xu, W. Lin, A fluorescent dyad with large emission shift for discrimination of cysteine/homocysteine from glutathione and hydrogen sulfide and the application of bioimaging, Anal. Chim. Acta 981 (2017) 86–93.
[3] X. Zhao, H. Ji, K. Hasrat, S. Misal, F. He, Y. Dai, F. Ma, Z. Qi, A mitochondria-targeted single fluorescence probe for separately and continuously visualizing H_2S and Cys with multi-response signals, Anal. Chim. Acta 1107 (2020) 172–182.
[4] G.I. Giles, K.M. Tasker, C. Collins, N.M. Giles, E. O'rourke, C. Jacob, Reactive sulphur species: an in vitro investigation of the oxidation properties of disulphide S-oxides, Biochem. J. 364 (2002) 579–585.
[5] G.I. Giles, K.M. Tasker, C. Jacob, Hypothesis: the role of reactive sulfur species in oxidative stress, Free Radical Biol. Med. 31 (2001) 1279–1283.
[6] J. Sun, Y. Bai, Q. Ma, H. Zhang, M. Wu, C. Wang, M. Tian, A FRET-based ratiometric fluorescent probe for highly selective detection of hydrogen polysulfides based on a coumarin-rhodol derivative, Spectrochim. Acta Part A 241 (2020) 118650.
[7] L. Li, M. Bhatia, Y.Z. Zhu, Y.C. Zhu, R.D. Ramnath, Z.J. Wang, F.B.M. Anuar, M. Whiteman, M. Salto-Tellez, P.K. Moore, Hydrogen sulfide is a novel mediator of lipopolysaccharide-induced inflammation in the mouse, Faseb J. 19 (2005) 1196–1198.
[8] K. Eto, T. Asada, K. Arima, T. Makifuchi, H. Kimura, Brain hydrogen sulfide is severely decreased in Alzheimer's disease, Biochem. Biophys. Res. Commun. 293 (2002) 1485–1488.
[9] T. Ida, T. Sawa, H. Ihara, Y. Tsuchiya, Y. Watanabe, Y. Kumagai, M. Suematsu, H. Motohashi, S. Fujii, T. Matsunaga, Reactive cysteine persulfides and S-polythiolation regulate oxidative stress and redox signaling, Proc. Natl. Acad. Sci. USA 111 (2014) 7606–7611.
[10] D. Zhang, I. Macinkovic, N.O. Devarie-Baez, J. Pan, C.M. Park, K.S. Carroll, M.R. Filipovic, M. Xian, Detektion von Persulfidbildung an Proteinen (S-Sulfhydrierung) mithilfe einer Tag-Switch-Technik, Angew. Chem. Int. Ed. 126 (2014) 586–592.
[11] K.M. Miranda, D.A. Wink, Persulfides and the cellular thiol landscape, Proc. Natl. Acad. Sci. USA 111 (2014) 7505.
[12] P. Nagy, M.T. Ashby, Reactive sulfur species: kinetics and mechanisms of the oxidation of cysteine by hypohalous acid to give cysteine sulfenic acid, J. Am. Chem. Soc. 129 (2007) 14082–14091.
[13] C. Wang, J. Xu, Q. Ma, Y. Bai, M. Tian, J. Sun, Z. Zhang, A highly selective fluorescent probe for hydrogen polysulfides in living cells based on a naphthalene derivative, Spectrochim. Acta Part A 227 (2020) 117579.
[14] C. Hwang, A.J. Sinskey, H.F. Lodish, Oxidized redox state of glutathione in the endoplasmic reticulum, Science 257 (1992) 1496–1502.
[15] A. Meister, M.E. Anderson, GLUTATHIONE, Annu. Rev. Biochem 52 (1983) 711–760.
[16] R. Greiner, Z. Pálinkás, K. Bäsell, D. Becher, H. Antelmann, P. Nagy, T.P. Dick, Polysulfides link H_2S to protein thiol oxidation, Antioxid. Redox Sign. 19 (2013) 1749–1765.
[17] K. Ono, T. Akaike, T. Sawa, Y. Kumagai, D.A. Wink, D.J. Tantillo, A.J. Hobbs, P. Nagy, M. Xian, J. Lin, Redox chemistry and chemical biology of H_2S, hydropersulfides, and derived species: implications of their possible biological activity and utility, Free Radical Biol. Med. 77 (2014) 82–94.
[18] J.L. Wallace, R. Wang, Hydrogen sulfide-based therapeutics: exploiting a unique but ubiquitous gasotransmitter, Nat. Rev. Drug Discov. 14 (2015) 329–345.
[19] L.H. Lash, Mitochondrial glutathione transport: physiological, pathological and toxicological implications, Chem. Biol. Interact. 163 (2006) 54–67.
[20] V.M. Hudson, Rethinking cystic fibrosis pathology: the critical role of abnormal reduced glutathione (GSH) transport caused by CFTR mutation, Free Radical Biol. Med. 30 (2001) 1440–1461.
[21] M. Gu, A. Owen, S. Toffa, J. Cooper, D. Dexter, P. Jenner, C. Marsden, A. Schapira, Mitochondrial function, GSH and iron in neurodegeneration and Lewy body diseases, J. Neurol. Sci. 158 (1998) 24–29.
[22] R. Njälsson, S. Norgren, Physiological and pathological aspects of GSH metabolism, Acta Paediatr. 94 (2005) 132–137.
[23] H. Sies, Glutathione and its role in cellular functions, Free Radical Biol. Med. 27 (1999) 916–921.
[24] A. Nadeem, S.K. Chhabra, A. Masood, H.G. Raj, Increased oxidative stress and altered levels of antioxidants in asthma, J. Allergy Clin. Immunol. 111 (2003) 72–78.
[25] C.G. Taylor, L.E. Nagy, T.M. Bray, Nutritional and hormonal regulation of glutathione homeostasis, Curr. Top. Cell. Regul. 34 (1996) 189–208.
[26] R. Janaky, K. Ogita, B. Pasqualotto, J. Bains, S. Oja, Y. Yoneda, C. Shaw, Glutathione and signal transduction in the mammalian CNS, J. Neurochem. 73 (1999) 889–902.
[27] R. Miyamoto, S. Koike, Y. Takano, N. Shibuya, Y. Kimura, K. Hanaoka, Y. Urano, Y. Ogasawara, H. Kimura, Polysulfides (H_2S_n) produced from the interaction of hydrogen sulfide (H_2S) and nitric oxide (NO) activate TRPA1 channels, Sci. Rep. 7 (2017) 1–10.
[28] H. Kimura, The physiological role of hydrogen sulfide and beyond, Nitric Oxide 41 (2014) 4–10.
[29] D.R. Linden, Hydrogen sulfide signaling in the gastrointestinal tract, Antioxid. Redox Sign. 20 (2014) 818–830.
[30] S. Koike, Y. Ogasawara, N. Shibuya, H. Kimura, K. Ishii, Polysulfide exerts a protective effect against cytotoxicity caused by t-buthylhydroperoxide through Nrf2 signaling in neuroblastoma cells, FEBS Lett. 587 (2013) 3548–3555.
[31] N.E. Francoleon, S.J. Carrington, J.M. Fukuto, The reaction of H_2S with oxidized thiols: generation of persulfides and implications to H_2S biology, Arch. Biochem. Biophys. 516 (2011) 146–153.
[32] T.V. Mishanina, M. Libiad, R. Banerjee, Biogenesis of reactive sulfur species for signaling by hydrogen sulfide oxidation pathways, Nat. Chem. Biol. 11 (2015) 457–464.
[33] M.C. Gruhlke, A.J. Slusarenko, The biology of reactive sulfur species (RSS), Plant Physiol. Biochem. 59 (2012) 98–107.
[34] O. Kabil, N. Motl, R. Banerjee, H_2S and its role in redox signalling, Biochim. Biophys. Acta Proteins Proteomics 2014 (1844) 1355–1366.
[35] P.K. Yadav, M. Martinov, V. Vitvitsky, J. Seravalli, R. Wedmann, M.R. Filipovic, R. Banerjee, Biosynthesis and reactivity of cysteine persulfides in signaling, J. Am. Chem. Soc. 138 (2016) 289–299.
[36] C. Liu, J. Pan, S. Li, Y. Zhao, L.Y. Wu, C.E. Berkman, A.R. Whorton, M. Xian, Capture and visualization of hydrogen sulfide by a fluorescent probe, Angew. Chem. Int. Ed. 50 (2011) 10327–10329.
[37] X. Chen, Y. Zhou, X. Peng, J. Yoon, Fluorescent and colorimetric probes for detection of thiols, Chem. Soc. Rev. 39 (2010) 2120–2135.
[38] X. Li, X. Gao, W. Shi, H. Ma, Design strategies for water-soluble small molecular chromogenic and fluorogenic probes, Chem. Rev. 114 (2014) 590–659.
[39] J. Chan, S.C. Dodani, C.J. Chang, Reaction-based small-molecule fluorescent probes for chemoselective bioimaging, Nat. Chem. 4 (2012) 973–984.
[40] J. Fan, M. Hu, P. Zhan, X. Peng, Energy transfer cassettes based on organic fluorophores: construction and applications in ratiometric sensing, Chem. Soc. Rev. 42 (2013) 29–43.
[41] L. Yuan, W. Lin, K. Zheng, L. He, W. Huang, Far-red to near infrared analyte-responsive fluorescent probes based on organic fluorophore platforms for fluorescence imaging, Chem. Soc. Rev. 42 (2013) 622–661.
[42] S. Zhang, H. Li, Q. Yao, S. Ghazali, J. Fan, J. Du, J. Wang, F. Gao, M. Li, H. Wang, C. Dong, X. Peng, A unique two-photon fluorescent probe based on ICT mechanism for imaging palladium in living cells and mice, Chin. Chem. Lett. 31 (2020) 2913–2916.
[43] Y.F. Kang, L.Y. Niu, Q.Z. Yang, Fluorescent probes for detection of biothiols based on "aromatic nucleophilic substitution-rearrangement" mechanism, Chin. Chem. Lett. 30 (2019) 1791–1798.
[44] Q. Fang, X. Yue, S. Han, B. Wang, X. Song, A rapid and sensitive fluorescent probe for detecting hydrogen polysulfides in living cells and zebra fish, Spectrochim. Acta Part A 224 (2020) 117410.
[45] W. Chen, E.W. Rosser, T. Matsunaga, A. Pacheco, T. Akaike, M. Xian, The development of fluorescent probes for visualizing intracellular hydrogen polysulfides, Angew. Chem. Int. Ed. 127 (2015) 14167–14171.
[46] Y. Hou, X.F. Yang, Y. Zhong, Z. Li, Development of fluorescent probes for hydrogen polysulfides by using cinnamate ester as the recognition unit, Sens. Actuat. B Chem. 232 (2016) 531–537.
[47] W. Chen, C. Liu, B. Peng, Y. Zhao, A. Pacheco, M. Xian, New fluorescent probes for sulfane sulfurs and the application in bioimaging, Chem. Sci. 4 (2013) 2892–2896.
[48] C. Zhang, Q. Sun, L. Zhao, S. Gong, Z. Liu, A BODIPY-based ratiometric probe for sensing and imaging hydrogen polysulfides in living cells, Spectrochim. Acta Part A 223 (2019) 117295.
[49] M. Gao, F. Yu, H. Chen, L. Chen, Near-infrared fluorescent probe for imaging mitochondrial hydrogen polysulfides in living cells and in vivo, Anal. Chem. 87 (2015) 3631–3638.
[50] Y. Fang, W. Chen, W. Shi, H. Li, M. Xian, H. Ma, A near-infrared fluorescence off-on probe for sensitive imaging of hydrogen polysulfides in living cells and mice in vivo, Chem. Commun. 53 (2017) 8759–8762.
[51] M. Gao, X. Zhang, Y. Wang, Q. Liu, F. Yu, Y. Huang, C. Ding, L. Chen, Sequential detection of superoxide anion and hydrogen polysulfides under hypoxic stress via a spectral-response-separated fluorescent probe functioned with a nitrobenzene derivative, Anal. Chem. 91 (2019) 7774–7781.
[52] W. Li, L. Wang, S. Yin, H. Lai, L. Yuan, X. Zhang, Engineering a highly selective probe for ratiometric imaging of H 2 S n and revealing its signaling pathway in fatty liver disease, Chem. Sci. 11 (2020) 7991–7999.
[53] Y. Zhang, J. Zhang, M. Su, C. Li, Rational molecular design of a reversible BODIPY-Based fluorescent probe for real-time imaging of GSH dynamics in living cells, Biosens. Bioelectron. 175 (2021) 112866.
[54] F. Zhang, J. Han, J. Wang, X. Li, Y. Wang, B. Wang, X. Song, A near-infrared fluorescent probe for hydrogen polysulfides detection with a large Stokes shift, Spectrochim. Acta Part A 242 (2020) 118755.

[55] W. Li, L. Wang, S. Yin, H. Lai, L. Yuan, X. Zhang, Engineering a highly selective probe for ratiometric imaging of H_2S_n and revealing its signaling pathway in fatty liver disease, Chem. Sci. 11 (2020) 7991–7999.
[56] W. Chen, A. Pacheco, Y. Takano, J.J. Day, K. Hanaoka, M. Xian, A Single fluorescent probe to visualize hydrogen sulfide and hydrogen polysulfides with different fluorescence signals, Angew. Chem. Int. Ed. 55 (2016) 9993–9996.
[57] J.L. Sartoretto, H. Kalwa, M.D. Pluth, S.J. Lippard, T. Michel, Hydrogen peroxide differentially modulates cardiac myocyte nitric oxide synthesis, Proc. Natl. Acad. Sci. USA 108 (2011) 15792–15797.
[58] X.P. She, X.G. Song, J.M. He, Role and relationship of nitric oxide and hydrogen peroxide in light/dark-regulated stomatal movement in Vicia faba, Acta Bot. Sin. (Engl. Transl.) 46 (2004) 1292–1300.
[59] H. Komatsu, T. Miki, D. Citterio, T. Kubota, Y. Shindo, Y. Kitamura, K. Oka, K. Suzuki, Single molecular multianalyte (Ca^{2+}, Mg^{2+}) fluorescent probe and applications to bioimaging, J. Am. Chem. Soc. 127 (2005) 10798–10799.
[60] L. Yuan, W. Lin, Y. Xie, B. Chen, S. Zhu, Single fluorescent probe responds to H_2O_2, NO, and H_2O_2/NO with three different sets of fluorescence signals, J. Am. Chem. Soc. 134 (2012) 1305–1315.
[61] G.C. Van de Bittner, C.R. Bertozzi, C.J. Chang, Strategy for dual-analyte luciferin imaging. In vivo bioluminescence detection of hydrogen peroxide and caspase activity in a murine model of acute inflammation, J. Am. Chem. Soc. 135 (2013) 1783–1795.
[62] M.D. Hammers, M.D. Pluth, Ratiometric measurement of hydrogen sulfide and cysteine/homocysteine ratios using a dual-fluorophore fragmentation strategy, Anal. Chem. 86 (2014) 7135–7140.
[63] J. Wang, B. Li, W. Zhao, X. Zhang, X. Luo, M.E. Corkins, S.L. Cole, C. Wang, Y. Xiao, X. Bi, Two-photon near infrared fluorescent turn-on probe toward cysteine and its imaging applications, ACS Sens. 1 (2016) 882–887.
[64] L.A. Stubbing, F.F. Li, D.P. Furkert, V.E. Caprio, M.A. Brimble, Access to 2-alkyl chromanones via a conjugate addition approach, Tetrahedron 68 (2012) 6948–6956.
[65] W. Chen, X. Yue, H. Zhang, W. Li, L. Zhang, Q. Xiao, C. Huang, J. Sheng, X. Song, Simultaneous detection of glutathione and hydrogen polysulfides from different emission channels, Anal. Chem. 89 (2017) 12984–12991.
[66] Y. Kim, S.V. Mulay, M. Choi, S.B. Yu, S. Jon, D.G. Churchill, Exceptional time response, stability and selectivity in doubly-activated phenyl selenium-based glutathione-selective platform, Chem. Sci. 6 (2015) 5435–5439.
[67] D.P. Murale, S.T. Manjare, Y.S. Lee, D.G. Churchill, Fluorescence probing of the ferric Fenton reaction via novel chelation, Chem. Commun. 50 (2014) 359–361.
[68] X.Y. Zhu, S.J. Liu, Y.J. Liu, S. Wang, X. Ni, Glucocorticoids suppress cystathionine gamma-lyase expression and H_2S production in lipopolysaccharide-treated macrophages, Cell. Mol. Life Sci. 67 (2010) 1119–1132.